

UC Berkeley

UC Berkeley Previously Published Works

Title

SPT-based probabilistic and deterministic assessment of seismic soil liquefaction triggering hazard

Permalink

<https://escholarship.org/uc/item/8m6245qg>

Authors

Cetin, K. Onder
Seed, Raymond B
Kayen, Robert E
et al.

Publication Date

2018-12-01

DOI

10.1016/j.soildyn.2018.09.012

Peer reviewed



SPT-based probabilistic and deterministic assessment of seismic soil liquefaction triggering hazard



K. Onder Cetin^{a,*}, Raymond B. Seed^b, Robert E. Kayen^b, Robb E.S. Moss^c, H. Tolga Bilge^d,
Makbule Ilgac^a, Khaled Chowdhury^{b,e}

^a Dept. of Civil Engineering, Middle East Technical University, Ankara, Turkey

^b Dept. of Civil and Environmental Engineering, University of California, Berkeley, CA, USA

^c California Polytechnic State University, San Luis Obispo, CA, USA

^d GeoDestek Ltd. Sti., Ankara, Turkey

^e US Army Corps of Engineers, South Pacific Division Dam Safety Production Center, Sacramento, CA, USA

ARTICLE INFO

Keywords:

Soil liquefaction
Earthquake
Seismic hazard
Cyclic loading
Standard penetration test
In-situ test
Probability

ABSTRACT

This study serves as an update to the Cetin et al. (2000, 2004) [1,2] databases and presents new liquefaction triggering curves. Compared with these studies from over a decade ago, the resulting new Standard Penetration Test (SPT)-based triggering curves have shifted to slightly higher CSR-levels for a given $N_{1,60,CS}$ for values of $N_{1,60,CS}$ greater than 15 blows/ft, but the correlation curves remain essentially unchanged at $N_{1,60,CS}$ values less than 15 blows/ft. This paper addresses the improved database and the methodologies used for the development of the updated triggering relationships. A companion paper addresses the principal issues that cause differences among three widely used SPT-based liquefaction triggering relationships.

1. Introduction

Empirical field-based frameworks for the assessment of seismic soil liquefaction triggering hazard continues to be the principal approach used in engineering practice. Three in-situ index test methods; the Standard Penetration Test (SPT), the Cone Penetration Test (CPT), and the measurement of in-situ Shear Wave Velocity (V_s) have reached a level of development in the field such that their usage has been applied worldwide. These three methods and the data supporting them are discussed in detail in the recent 2016 report of the National Academies Sciences, Engineering, and Medicine, Committee on Geological and Geotechnical Engineering (COGGE): “State of the Art and Practice in the Assessment of Earthquake-Induced Soil Liquefaction and its Consequences”, (NAP [3]). Advances in test procedures in a fourth method, the Becker Penetration Test (BPT) may expand the test's usage in the future. New methods are under development, though these four tests remain the cornerstone of empirical test methodologies.

The authors used the opportunity presented by the NAP committee report to re-evaluate, organize, update the database of Cetin et al. [2] (hereafter, CEA2004), and then cast new regression models for seismic soil liquefaction triggering based on the data improvements.

2. Updated Cetin et al. [4,9] database

The case histories of CEA2004 are re-visited so as to correct errors in the original document, as well as take advantage of updates in the current state of knowledge. Changes to the database include the following:

- (1) A typographical error at the third decimal point in the spreadsheet execution of the r_d formula in the original work of Cetin et al. [2] was identified. This error biased r_d values towards the low side. The effect was negligible at the ground surface and increased with depth. The overall average increase in the new r_d values for the 150 affected case histories was 6.1%. The remaining 50 field performance case histories had r_d values directly calculated from site-specific and event-specific seismic site response analyses (Cetin et al. [1], Cetin [5]). Since these 50 r_d values were properly estimated in the original database, they simply remain unchanged. A brief discussion of the consistent use of Cetin and Seed [6] r_d relationship will be presented later in this manuscript, and a more detailed discussion is available in Cetin et al. [7]. The estimation of r_d values in Cetin and Seed [6] requires the estimation of representative shear wave velocity in the upper 12 m of

* Corresponding author.

E-mail addresses: kemalondercetin@gmail.com, ocetin@metu.edu.tr (K.O. Cetin).

Nomenclature

a_{\max}	peak horizontal acceleration	$N_{1,60}$	standard penetration test blowcount value corrected for overburden, energy, equipment and procedural factors
C_B	SPT correction for borehole diameter	$N_{1,60,cs}$	finer-corrected $N_{1,60}$ value
C_E	SPT correction for hammer energy ratio (ER)	$\Delta N_{1,60}$	SPT penetration resistance correction for fines content
C_N	overburden correction factor	M	earthquake magnitude
C_R	SPT correction factor for the rod length	M_w	earthquake moment magnitude
C_S	SPT correction for sampler configuration details	M_L	earthquake local magnitude
CSR	cyclic stress ratio	M_s	earthquake surface wave magnitude
$CSR_{\sigma'_v=1 \text{ atm}, \alpha=0, M_w=7.5}$	CSR normalized to $\sigma'_v = 1 \text{ atm}$, $M_w = 7.5$ and $\alpha = 0$	P_a	atmospheric pressure (1 atm)
$CSR_{\sigma'_v=1 \text{ atm}, M_w=7.5}$	CSR normalized to $\sigma'_v = 1 \text{ atm}$, $M_w = 7.5$	P_L	probability of triggering of liquefaction
$CSR_{\sigma'_v, \alpha, M_w}$	actual CSR, not normalized to a reference state of $\sigma'_v = 1 \text{ atm}$, $M_w = 7.5$ and $\alpha = 0$	PI	plasticity index
$CSR_{\sigma'_v, M_w}$	actual CSR, not normalized to a reference state of $\sigma'_v = 1 \text{ atm}$, $M_w = 7.5$	r_d	shear mass modal participation factor, commonly referred to as cyclic shear stress reduction factor
$CSR_{\text{peak}, \sigma'_v, M_w}$	peak CSR, not normalized to a reference state of $\sigma'_v = 1 \text{ atm}$, $M_w = 7.5$	SPT-N	standard penetration test blow count
CRR	cyclic resistance ratio	W_{liq}	corrective weighting factor for the liquefied data
$d_{cr} = d$	critical depth for liquefaction	W_{nonliq}	corrective weighting factor for the non-liquefied data
D_R	relative density	V_s	shear wave velocity
FC	fines content	$V_{s,12 \text{ m}}$	shear wave velocity for the upper 12 m
FS	factor of safety against triggering of liquefaction	γ_{sat}	unitweight below ground water table
g	acceleration of gravity	γ_{moist}	unitweight above ground water table
H_i	thickness of soil sublayers		standard deviation
K_{M_w}	correction for magnitude (duration) effects	σ_ϵ	standard deviation of the model uncertainty
K_σ	correction for overburden stress	Φ	standard cumulative normal distribution
K_α	correction for sloping sites	φ	standard normal density function
N	field measured standard penetration resistance (blows/30 cm)	ϵ	model error term
N_{60}	standard penetration test blowcount value corrected for energy, equipment and procedural factors	σ_ϵ, r_d	standard deviation of the model uncertainty of r_d
N_1	standard penetration test blowcount value corrected for overburden.	σ'_v	vertical effective stress
		σ_v	vertical total stress
		θ	limit state model coefficient
		Θ	set of unknown model coefficients
		$\Delta N_{1,60}$	SPT penetration resistance correction for fines content
		α	initial static driving shear stress ratio; $\alpha = \tau_{hv,static} / \sigma'_v$
		γ_{\max}	maximum shear strain

the soil profile. Compared to the earlier version of the database, shear wave velocities for the 150 cases increased on average 6.6%. The changes to V_s had a negligible impact on the estimated r_d values, however they were performed for consistency by following the recommendations of Japan Road Association [8]. Fig. 1 presents a visual comparison between the back-analyzed field performance case history input parameters of the CEA2004 and Cetin et al. [4,9] databases. In this figure, the black and red symbols represent the values from CEA2004 and Cetin et al. [4,9], respectively.

- (2) Unit weights for each case history site were updated as given in Table 1, unless the available case-specific information was indicating otherwise. Individual unit weights for each case, and each stratum, typically vary slightly based on information available. Details for each case history are presented in Cetin et al. [4,9]. The updated unit weights are, typically, very close to, and slightly lower than, the average values common to the databases of Cetin et al. [4,9] and Idriss and Boulanger [10] (hereafter IB2010). In the average, the γ_{moist} and $\gamma_{\text{saturated}}$ values increased by approximately 10% as compared to the values used in CEA2004. Mean values of the unit weights used for case history processing will be presented later in the manuscript. The changes in unit weight affect the values of total and effective stresses.
- (3) The conversion of atmospheric pressure (P_a) from atmospheres to kilopascals to pounds-per-square-foot was set accurately as follows for all case histories: $1 \text{ atm} \cong 101.3 \text{ kPa} \cong 2116.2 \text{ lbs/ft}^2$. In CEA2004, these conversions which are needed for the effective stress adjustments (C_N) to SPT blow counts and K_σ adjustments for cyclic stress ratio were approximated as $1 \text{ atm} = 100 \text{ kPa} = 2000 \text{ lbs/ft}^2$. These adjustments and updates were common to all case

histories.

Some modifications were made to selected case histories per observations of Idriss and Boulanger [11]. The authors excluded three cases from the CEA2004 database: (1) 1975 Haicheng Earthquake ($M_s = 7.3$) Shung Tai Zi River, (2) 1994 Northridge Earthquake ($M_w = 6.7$) Malden Street Unit D, and (3) 1979 Imperial Valley Earthquake ($M_L = 6.6$) Wildlife Unit B. The reasons for exclusion of these cases are summarized in Table 2.

Three case history sites (1) 1989 Loma Prieta Earthquake ($M_w = 6.93$) Clint Miller Farm (CMF-10), and 1995 Hyogoken-Nanbu Earthquake ($M_w = 6.9$) Kobe (2) # 6 and (3) #16 are now reclassified as non-liquefaction sites. Additionally, (4) the critical depth of the 1993 Kushiro-Oki Earthquake ($M_w = 7.6$) Kushiro Port strong motion recording station case history site is modified. The reasons for the modifications of these cases are summarized in Table 3.

Recent work on ground motion models and, in particular, the database development of the Next Generation Attenuation (NGA) project, has provided new insight into some of the historical earthquake magnitudes and, therefore, estimated peak ground acceleration levels. New moment magnitudes for events are summarized in Table 4, and they are compared with the moment magnitudes used in CEA2004. Changes in moment magnitudes are relatively minor and were made for completeness. The changes to magnitude had a negligible impact on the triggering correlations.

All other cases were also reviewed, and for some cases, details such as the elevation of the phreatic surface, a_{\max} , average fines content, critical depth, average SPT-N values, C_R and/or C_B corrections were reassessed and adjusted. As shown in Fig. 1, resulting modifications here

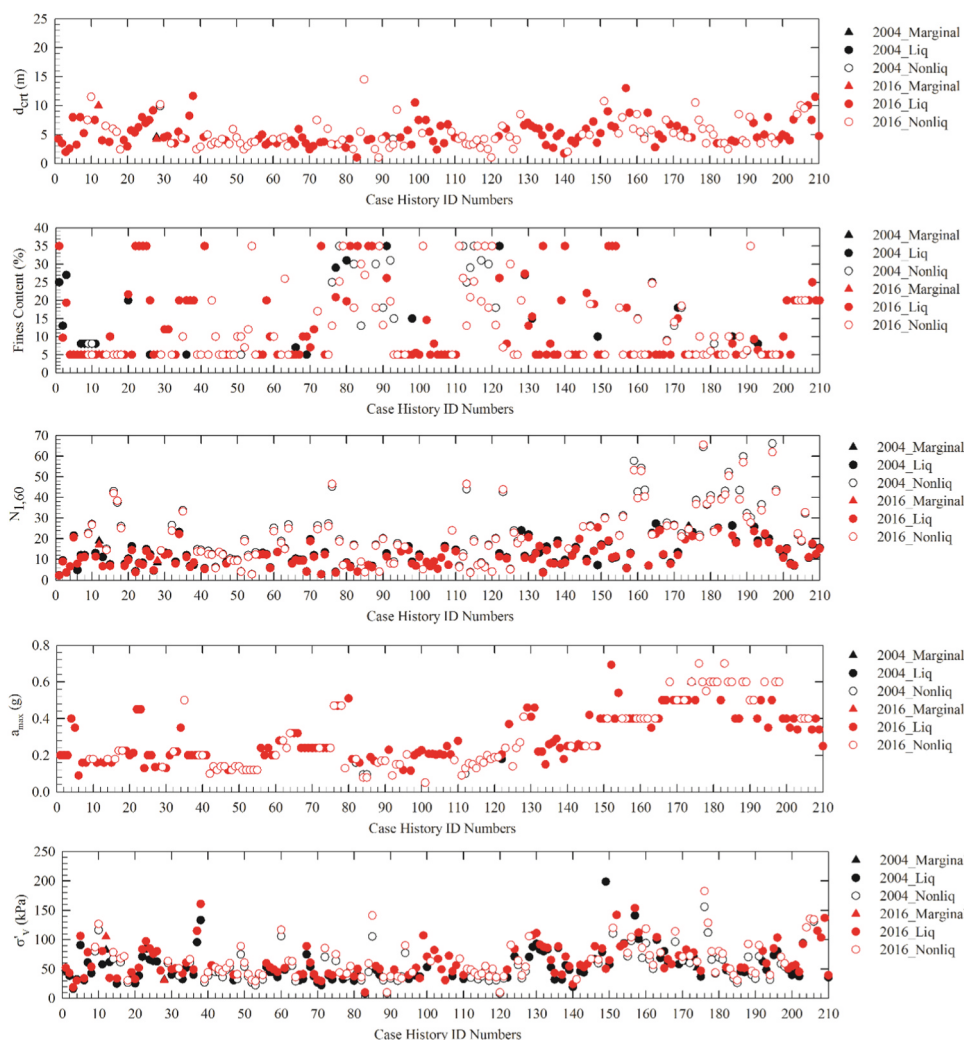


Fig. 1. Comparison of case history model input parameters (a) d_{crit} (b) Fines content (c) $N_{1,60}$ (d) a_{max} (e) σ'_v for CEA2004 and Cetin et al. [4,9]. (Case histories are numbered as listed in Table S1). Comparison of case history model input parameters for CEA2004 and Cetin et al. [4,9]. (f) σ_v (g) V_s (h) r_d (i) M_w (j) CSR. (Case histories are numbered as listed in Table S1).

were typically minor and had no significant impact on the resulting liquefaction triggering correlations developed.

The IB2010 SPT-catalog database has 230 case histories, and many are those screened and compiled by CEA2004. A new group of 33 case histories was added by IB2010. These include twenty seven case histories compiled by Iai et al. [21] for the 1983 Nihonkai-Chubu Earthquake ($M = 7.7$), three case histories from the 1989 Loma Prieta Earthquake ($M_w = 6.93$), one from the 1964 Niigata Earthquake ($M_w = 7.6$), one from the 1968 Hyūga-nada Earthquake ($M = 6.9$), and one from the 1982 Urakawa-Oki Earthquake ($M = 6.9$). More recently, Boulanger and Idriss [22] (hereafter BI2014) compiled 24 additional cases from the 1999 Kocaeli ($M_w = 7.51$) and 1999 Chi-Chi ($M_w = 7.62$) earthquakes.

Cetin et al. [4,9] re-evaluated these 57 new cases. The screening criteria used for the CEA2004 were used here, and 13 of the new IB2010 and BI2014 case histories (10 of the Nihonkai-Chubu and 3 of the Loma Prieta earthquake case histories) satisfied the authors screening criteria, and were added to the database presented here. These 13 new cases added are listed in Table 5. Non-inclusion of the remaining case histories is discussed in Cetin et al. [4,9] and these exclusions were consistent with the criteria used to assess the authors' original database: that is, due to not meeting one or more of the following screening filters: (1) soil profiles (e.g.: boring logs) are not well documented or accessible, (2) soil properties for the critical soil layer

are not available to assess plasticity, (3) sites are not free-field, due to non-level topography or close proximity of a structure, and (4) the use of percussion drilling techniques for SPT borings.

2.1. Summary of changes to the new database

The updated database is schematically presented in Fig. 2, and plotted here as the mean values of $CSR_{\sigma'_v, M_w}$ and $N_{1,60}$ for each case history, without fines corrections, or adjustments for effective stress (K_G) and earthquake magnitude (K_{M_w}). In Fig. 2, “Seed et al.” represents cases from Seed et al. [21]. The 1995 Hyogoken-Nanbu Earthquake (“Kobe EQ”) cases are from the CEA2004 database. “Cetin et al.” data points represent the remaining case histories. The database is also summarized in Supplementary material Table S1. A complete discussion of the case history database, its background documentation, analysis, and parametric evaluations are available in Cetin et al. [4,9].

In Table 6, there is a comparative summary of key database statistics of Seed et al. [23], CEA2004, Cetin et al. [4,9] and IB2010. While calculating these composite statistics for all three of these databases (1) liquefied, (2) nonliquefied, and (3) Hyogoken-Nanbu (Kobe) earthquake case histories were each weighted individually as will be discussed later in this manuscript. So the cross-comparisons here are based on identical weighting within each database. As a result, the parameter ensemble averages shown in Table 6 are not biased by different

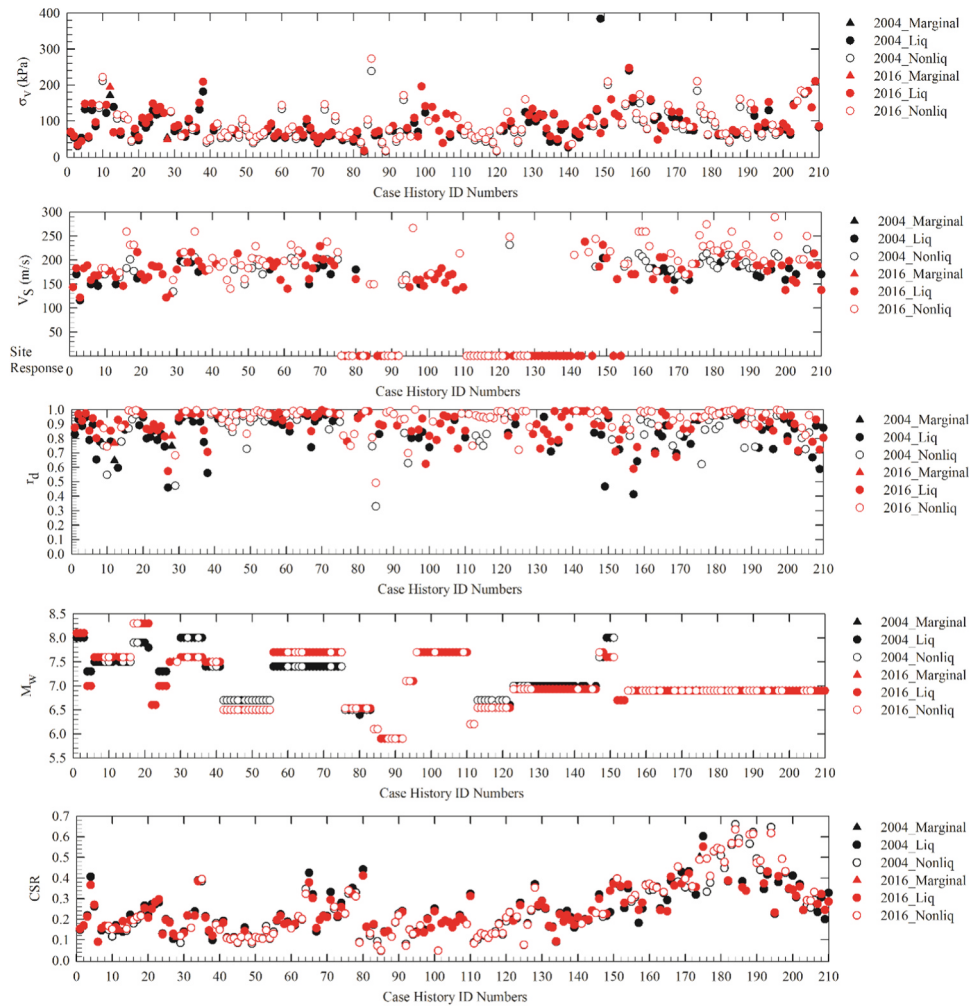


Fig. 1. (continued)

Table 1
Assumed unit weights as used in Cetin et al. [4,9] for back analyses of field performance case histories unless case-specific values are available.

(a) Coarse-grained soil layers				
SPT-N ₆₀ (blows/ft)	γ _{moist}		γ _{sat}	
	(lb/ft ³)	(kN/m ³)	(lb/ft ³)	(kN/m ³)
0–4	100	15.7	110	17.3
5–10	110	17.3	120	18.9
11–30	120	18.9	125	19.6
30–50	125	19.6	135	21.2
(b) Fine-grained soil layers				
0–4	100	15.7	110	17.3
5–8	110	17.3	120	18.9
9–16	115	18.1	125	19.6

weighting schemes, and direct cross-comparisons are, therefore, meaningful.

Interestingly, in the calculation of cyclic stress ratios (CSR), the effect of the average increase in r_d values in the new database of Cetin et al. [4,9], relative to CEA2004, is largely offset by the effect of increased unit weight has on the ratio of σ_v / σ'_v . The effect of this offset is seen in the final plot of Fig. 1(j), where the updated $CSR_{\sigma'_v, M_{10}}$ values are likely to decrease in nearly as many cases as those for which there is an increase.

3. Conventions for analyzing liquefaction field performance case histories

The key elements of the conventions and procedures employed in the authors' evaluation of the field performance case histories for this study are essentially the same as those employed in Cetin et al. [1,2]. Additional descriptions and details are provided by Cetin [5] and some of these are also discussed in the companion manuscript of Cetin et al. [24] and Cetin et al. [7].

3.1. Case history screening

All case histories used in these studies are free-field and level ground cases. Cases with ground slopes greater than 3%, or cases near a free face (e.g. trench, stream cut, shoreline etc.) were eliminated. Cases in which soil/structure interaction might have had a pronounced influence on the cyclic shear stress, or enhanced liquefaction damage, were eliminated. Case histories can produce only binary outcomes- sites either liquefied or not. The authors made exceptions for two case histories where the performance was characterized as "marginal" by the field team that made the observation. There is only one single most 'critical layer' at any borehole, and it was not allowed to evaluate both "liquefied" and "non-liquefied" data for the same borehole (or the same site, if multiple borings characterize the same soil unit), as the onset of liquefaction in one stratum reduces cyclic shear stresses in both overlying and underlying strata such that back-analyses for other layers become unreliable. That is, deriving an unbiased "non-liquefied" data

Table 2
Reasons for exclusion of the three case histories.

Case history	Comments
1975 Haicheng Earthquake ($M_s = 7.3$), Shuang Tai Zi River	Lack of documentation of fines content and soil texture limits in the original reference. This information is needed to judge if the suspect fine grained soil layer is non-plastic or not. Seed et al. [12] described the critical layer as "silt" with no further details.
1994 Northridge Earthquake ($M_w = 6.7$), Malden Street Unit D	Unit A is a compacted fill, located mostly above the water table, and is judged to be non-liquefiable; Unit B is a fine grained soil layer with $N \approx 2-3$ blows/ft., and $FC > 70\%$, with average $PI = 18\%$, and average clay content of 31% (Bennett et al. [13]). Clayey soils with $PI = 18\%$, were categorically judged to be non-liquefiable in Cetin [5] and CEA2004. Unit D is Pleistocene silty sand. However, revisiting this case history based on exchanges with the original field investigators, it has been determined that the suspect layer for the observed ground deformations is the soft fine-grained plastic Unit B that accumulated permanent seismic displacements during the dynamic loading of cohesive soils, as proposed and modeled recently by Kayen [14].
1979 Imperial Valley Earthquake ($M_L = 6.6$), Wildlife Unit B	Lack of a confirmed no-liquefaction performance by field investigators. Youd [15] noted that: "the no assigned to the Wildlife site for the 1979 Imperial Valley Earthquake ($M = 6.5$) was not confirmed by investigator observation."

point from other strata at a site where one or more strata have liquefied, is not possible. Compiling multiple case histories from a single borehole also has the negative effect of weakening the statistical independence of the maximum likelihood formulation. At each case history site, the critical stratum was identified as the non-plastic, submerged soil substratum most susceptible to triggering of liquefaction, and the mid-depth of the critical sub-layer was used as the representative depth. However, soil properties were assessed within the full thickness of the critical soil layer.

3.2. Estimation of the CSR

Peak ground surface acceleration (a_{max}) values for each case history were estimated using source mechanism and geometry, local and regional recorded strong motion data, and suites of available ground motion prediction equations. When available, values of a_{max} in the database are estimated as the geometric mean (GM) of the two orthogonal peak ground acceleration (PGA) horizontal components (i. e. $GM = \sqrt{PGA_1 \cdot PGA_2}$) of motion. However, if the geometric mean of the rotated set of components corresponding to pp^{th} percentile (i.e.: $GMRotDpp$) is available, a suitable conversion factor needs to be applied. Uncertainty (or variance) in a_{max} was evaluated for each case and is directly reflective of the level and quality of data for each case history.

For 48 of the 210 liquefaction field performance case histories, in-situ $CSR_{\sigma'_v, M_w}$ was evaluated based on site-specific and event-specific seismic site response analyses (using SHAKE 91; Idriss and Sun [25]). For the remaining 162 cases, wherein full seismic site response analyses were not performed, $CSR_{\sigma'_v, M_w}$ was evaluated using the estimated a_{max} and Eq. (1), with r_d -values estimated by using the predictive r_d relationship developed by Cetin and Seed [6,26].

Table 3
Reasons for the modification of four case histories.

Case History ID	Comments
1989 Loma Prieta Earthquake ($M_w = 6.93$), Miller Farm CMF-10	At the time of Cetin [5] and CEA2004 studies, the Clint Miller Farm CMF-10 case history site was classified as a liquefied site. The CMF-10 borehole was located in a suite of tests across a permanent deformation transition zone and it is now understood that the field investigation team (Wayne et al. [16]) intended CMF-10 to represent the non-liquefied zone. The authors accept the field judgments of the field investigation teams.
1995 Hyogoken-Nanbu Earthquake ($M_w = 6.9$), Kobe # 6	This site was found to be inconsistently listed as a non-liquefied and a liquefied site on the summary table and the map, respectively, from the Kobe City Office in 1999. After personal communication with Prof. Tokimatsu, the site is updated as a "non-liquefied" site.
1995 Hyogoken-Nanbu Earthquake ($M_w = 6.9$), Kobe # 16	Due to the proximity of Kobe #15 (Liquefied) and #16 (Non-Liquefied) sites, Kobe # 16 was originally classified as a marginal liquefaction (Yes/No) site. Now it is treated as a non-liquefied site.
1993 Kushiro-Oki Earthquake ($M_w = 7.6$), Kushiro Port strong motion recording station	When the CEA2004 database was compiled, the silty layer at the depth range of 20–22 m with SPT-N values of 6–10 blows/ft was judged to be the suspect stratum. However, after having revisited this case history, the suspect stratum was identified as "medium dense" coarse sand soil layer with SPT-N values of 16–18 blows/ft at the depth range of 2.8–5.2 m. This case history is judged to warrant further in depth investigation. Meanwhile, this shallower "medium dense" coarse sand soil layer is used as the critical layer.

Table 4
Comparison between the moment magnitudes (M_w) used in CEA2004 and Cetin et al. [4,9].

Earthquake	CEA2004	Cetin et al. [4,9]	Ref.
1944 Tohankai	8.00	8.10	USGS Centennial Earthquake Catalog, Engdahl and Villasenor [17]
1948 Fukui	7.30	7.00	
1968 Tokachioki	7.90	8.30	
1975 Haicheng	7.30	7.00	
1976 Tangshan	8.00	7.60	NGA Flatfiles [18]
1977 Argentina	7.40	7.50	
1978 Miyagiken-Oki Feb. 20	6.70	6.50	
1978 Miyagiken-Oki June 12	7.40	7.70	
1990 Luzon	7.60	7.70	Incorporated Research Institutions for Seismology (IRIS) Seismo Archives [19] Ide and Takeo [20]
1979 Imperial Valley	6.50	6.53	
1987 Superstition Hills	6.70	6.54	
1989 Loma Prieta	7.00	6.93	
1964 Niigata	7.50	7.60	
1993 Kushiro-Oki	8.00	7.60	

$$CSR_{\sigma'_v, M_w} = 0.65 \cdot CSR_{peak, \sigma'_v, M_w} = 0.65 \cdot \frac{a_{max}}{g} \cdot \frac{\sigma'_v}{\sigma'_v} \cdot r_d \tag{1}$$

In Eq. (3), as defined earlier, a_{max} is the peak horizontal ground surface acceleration; g is the acceleration of gravity, σ'_v and σ'_v are total and effective vertical stresses, respectively, and r_d is the stress reduction or nonlinear shear mass participation factor. A full explanation of the development of the probabilistic r_d relationship is presented in Cetin and Seed [6,24]. In total, 2153 one-dimensional seismic site response

Table 5
List of 13 additional field performance case histories from IB2010 that were added to Cetin et al. [4,9] database.

1983 Nihonkai-Chubu M = 7.7 Earthquake	1989 Loma Prieta M _w = 6.93 Earthquake
1. Akita Station	1. General Fish
2. Gaiko 1&2	2. Marina Laboratory_F1-F7
3. Hakodate	3. MBARI NO.4-B4B5EB2EB3
4. Nakajima No. 1(5)	
5. Nakajima No. 2(1)	
6. Nakajima No. 2(2)	
7. Nakajima No. 3(3)	
8. Nakajima No. 3(4)	
9. Ohama No. 2(2)	
10. Ohama No. Rvt. (1)	

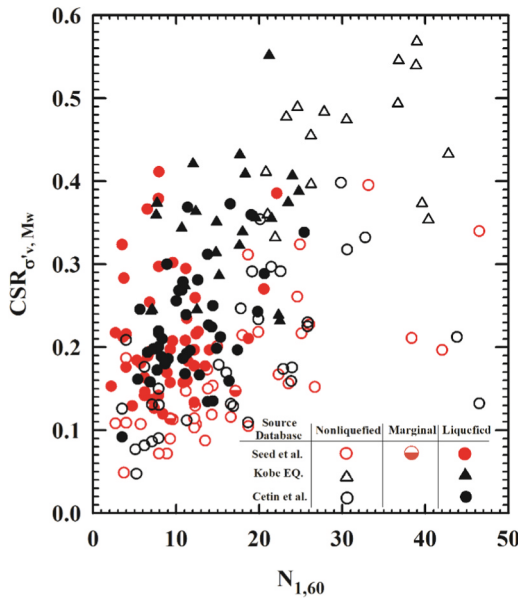


Fig. 2. Summary of the Cetin et al. [4,9] field performance case history data.

Table 6
Summary and comparison of overall case history weighted average input parameters.

Parameter	Seed et al. [10] 125 case history		CEA2004 200 case history		Cetin et al. [4,9] 210 case history		IB2010 230 case history	
	Mean	Mean Std. Dev.	Mean	Mean Std. Dev.	Mean	Mean Std. Dev.	Mean	Mean Std. Dev.
γ _{moist} (kN/m ³)	–	–	15.2	0.67	16.77	0.47	–	–
γ _{saturated} (kN/m ³)	–	–	16.91	0.69	18.91	0.47	–	–
Critical Depth: d _{cr} (m)	5.80	–	5.08	0.53	4.93	0.55	5.02	–
N _{1,60}	13.51	–	15.83	3.15	15.13	3.09	15.02	–
FC (%)	14.72	–	18.89	3.02	16.57	4.16	16.24	–
ΔN _{1,60}	–	–	1.61	^a	1.52	^a	1.94	–
N _{1,60,CS}	–	–	17.44	^a	16.65	^a	16.96	–
a _{max} (g)	0.22	–	0.25	0.04	0.24	0.05	0.25	–
σ _v (kPa)	105.58	–	83.87	9.52	89.70	10.60	91.78	–
σ' _v (kPa)	67.45	–	53.48	5.83	60.62	5.62	61.29	–
V _{s,12 m} (m/s)	–	–	178.92	–	190.87	–	–	–
r _d	0.953	–	0.859	0.058	0.911	0.057	0.949	–
CSR _{σ'_v,M_w}	0.210	–	0.211	0.04	0.208	0.05	0.225	–
M _w	7.12	–	7.06	–	7.09	–	7.13	–
K _{Mw}	–	–	1.17	–	1.17	–	1.12	–
K _σ	–	–	1.23	–	1.25	–	1.06	–
CSR _{σ'_v=1 atm, M_w=7.5}	0.197	–	0.158	–	0.156	–	0.196	–

^a Functions of regressed likelihood model coefficients, as presented later in this manuscript.

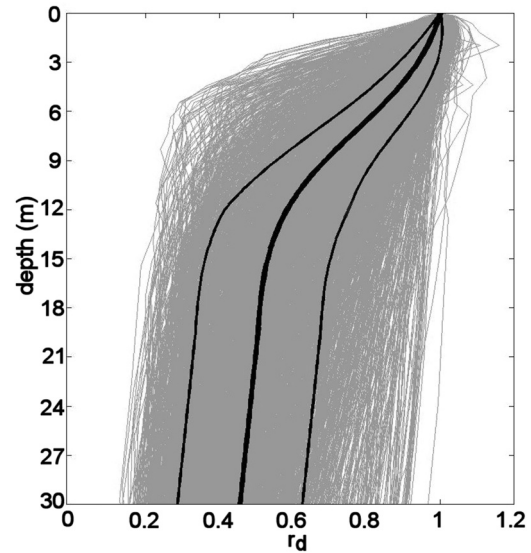


Fig. 3. Plots of r_d for all 2153 site response analyses for all combinations of sites and input motions superimposed with the predictions based on group mean values of V_s, M_w, and a_{max} (Heavy black lines show regressed mean and ± 1 standard deviations) (taken from Cetin and Seed [6]).

analyses were performed in order to generate the data set for probabilistic regressions. Fig. 3 shows the r_d curves for all of these site response analyses.

The consistent use of r_d relationship of Cetin and Seed [6,26] is presented on an illustrative seismic soil liquefaction triggering assessment problem in Cetin et al. [7]; hence will not be repeated herein.

The probabilistic regressions indicate that the harder a soil column is shaken, and the softer the column is, the greater the degree of non-linearity of response that results, such that r_d values decrease more rapidly with increasing depth. Increased heterogeneity or distinct “layering” of the site conditions tends to break up wave coherence, and also tends to cause r_d values to decrease more rapidly with increasing depth. Increased magnitude serves as a proxy for duration, and is the least significant of the four factors. The predictive relationship of Cetin and Seed [6,26] is intended to be used on soil profiles with potentially liquefiable layers and it is recommended by the authors that an upper bound of V_{s,12 m} ≤ 230 m/s be employed in forward analyses so as not

to produce nearly rigid body type response predictions. The shear wave velocity value of 230 m/s for $V_{S,12\text{ m}}$ is coincident with the zone of highest values of V_{S1} found to have liquefied in the database of Kayen et al. [27]. Similarly, for unusually soft sites with $V_{S,12\text{ m}} \leq 90$ m/s, r_d relationship of Cetin and Seed [6,26] can be employed, though that lower value of average shear wave velocity corresponds with the very lowest V_{S1} reported in Kayen et al. [27]. No site exists with conditions of $V_{S,12\text{ m}}$ less than 90 m/s or above 230 m/s in any of the liquefaction databases, though these studies represent the vast majority of well documented field-performance sites. $V_{S,12\text{ m}}$ is estimated by calculating the apparent travel times through each sub-layer, down to a depth of 12 m, and then by dividing the total distance (i.e.: 12 m) by the total travel time. A detailed discussion on consistent estimation of $V_{S,12\text{ m}}$ is presented in Cetin et al. [7] by an illustrative seismic soil liquefaction triggering assessment problem; hence will not be repeated herein.

These approaches were employed to develop unbiased best-estimates of r_d , and its variance. As such, the resulting liquefaction triggering relationships can be used in forward engineering analyses with either r_d relationship of Cetin and Seed [6,26], or site-specific seismic site response analyses. Factors contributing to overall variance in estimation of the equivalent uniform cyclic shear stress ratio ($CSR_{\sigma'_v, M_w}$) were summed within a structural reliability framework. The main contributors to this variance were (1) uncertainty in a_{max} , and (2) uncertainty in nonlinear shear mass participation factor (or r_d). Other variables, which contributed to a lesser degree to the overall variance were the depth of the critical soil stratum, soil unit weights, and location of the phreatic surface (“water table depth”) at the time of the earthquake.

3.3. Estimation of SPT-N values

Some case histories have critical layers characterized with only a single SPT boring, while others have dense concentrations characterized from multiple SPT borings. This study assigned a single case history to the total number of borings at the same site that could be grouped together to jointly define a stratum. Cases with more SPT data usually have lower uncertainties in their N-values. These cases exert more weight on the location of the triggering curves than less well-characterized cases with higher uncertainty.

The resulting $N_{1,60}$ values are the product of the averaged N values for a stratum corrected for effective normal stress (C_N), hammer energy (C_E), equipment rod length (C_R), equipment sampler (C_S), borehole diameter (C_B), and procedural effects to fully standardized $N_{1,60}$ values as given in Eq. (2).

$$N_{1,60} = N \cdot C_N \cdot C_R \cdot C_S \cdot C_B \cdot C_E \quad (2)$$

The corrections for C_N , C_R , C_S , C_B and C_E correspond closely to those recommended by the NCEER Working Group (NCEER [28], and Youd et al. [29]), and are discussed in CEA2004 and Cetin et al. [4,7]; hence will not be repeated herein. In the literature there exist alternative correction schemes regarding these factors (e.g. effective stress only or effective stress and relative density dependent C_N (Liao and Whitman [30], Boulanger [31], etc.) or rod length (NCEER workshop proceedings [28], CEA2004, Sancio and Bray [32], etc.). However, due to lack of consensus among these correction schemes, and due to their relative insignificance on the overall corrected SPT blow counts, NCEER workshop consensus recommendation is adopted. For effective stress ranges exceeding 2 atm, which is outside the limits of case history-based liquefaction triggering models, the differences between effective stress only-, and effective stress-relative density dependent- C_N correction schemes can be significant. Hence, their effects on the estimated $N_{1,60}$ values should be carefully and case specifically assessed. For further discussion regarding these correction factors refer to NCEER Workshop Proceedings [28], Youd et al. [29], CEA2004 and Cetin et al. [4,9].

For 20 out of 210 cases wherein the critical stratum had only one

single useful $N_{1,60}$ -value, the standard deviation was taken as 2 blows/ft because 2 blows/ft was typical of the larger variances among the cases with multiple $N_{1,60}$ values regardless of the value of the mean blow-count.

4. Development of probabilistic liquefaction triggering curves

Liquefaction triggering correlations were developed based on probabilistic “regressions” performed employing the maximum likelihood estimation (MLE) method. The formulations and approaches employed are described in detail by Cetin [5], Cetin et al. [4,33], and here only briefly. The MLE serves essentially the same purpose as multi-dimensional probabilistic “regression” analyses, but (1) allows for separate treatment of various contributing sources of aleatory uncertainty, and (2) facilitates treatment of more descriptive variables (model parameters) while also permitting the monitoring of model parameter interactions and co-variances. Within the MLE analyses, all data (i.e.: CSR , $N_{1,60}$, σ'_v , FC , M_w) were modeled as random variables. Thus, the points in Figs. 1 and 2 are actually the mean values of uncertainty clouds in all parametric directions for each case history.

All liquefaction databases have a sampling disparity that biases the data set toward liquefied sites and is due to the undersampling of nonliquefied sites. Cetin et al. [1,2,33] proposed a procedure to balance the dataset by up-weighting the value of non-liquefied sites by a weighting factor of 1.2, and by down-weighting the value of liquefied sites by a factor of 0.8. This is approximately equivalent to simply up-weighting the non-liquefied cases by a factor of 1.5. However, partitioning the weighting factors among both liquefied and non-liquefied cases allows improved treatment of model uncertainty.

The Cetin et al. [4,9] database has nearly the same overall characteristics (and almost the same cases) as the CEA2004 database, and the same weighting factors (1.2 and 0.8) were again applied to liquefied and nonliquefied case histories. An additional weighting factor was needed to address the large number of case histories from the 1995 Hyogoken-Nanbu (Kobe, Japan) earthquake. The database has 56 case histories from this single event; and that very large number results in an unbalance of the overall data set wherein that single event is over-represented. This was addressed in the assessments performed for Cetin et al. [4,9] database by down-weighting the Hyogoken-Nanbu (Kobe) earthquake case histories by a weighting factor of 0.25. Additional details of the assessments performed are presented in Cetin et al. [4,9].

The maximum likelihood approach begins with the selection of a mathematical model. The model for the limit-state function has the general form $g = g(\mathbf{x}, \Theta)$, where $\mathbf{x} = (N_{1,60}, CSR_{\sigma'_v, \alpha, M_w}, M_w, FC, \sigma'_v)$ is a set of descriptive variables and Θ is the set of unknown model coefficients. Consistent with the normal definition of failure in structural reliability, liquefaction is assumed to have occurred when $g(\mathbf{x}, \Theta)$ takes on a negative value. The limit-state surface $g(\mathbf{x}, \Theta) = 0$ denotes the 50-percentile (median) boundary condition between liquefaction and nonliquefaction. The following model from Cetin et al. [2,33] is used for the limit state function:

$$g(\mathbf{x}, \Theta) = N_{1,60}(1 + \theta_1 FC) - \theta_2 \ln(M_w) - \theta_3 \ln\left(\frac{\sigma'_v}{P_a}\right) + \theta_4 FC + \theta_5 - \theta_6 \ln(CSR_{\sigma'_v, \alpha, M_w}) \quad (3)$$

where $\Theta = (\theta_1, \dots, \theta_6)$ is the set of unknown model coefficients.

The limit state function given in Eq. (3) has the advantage of assessing K_σ , K_{M_w} and fines corrections within a unified framework. Hence, as part of the maximum likelihood assessment, the overall liquefaction triggering relationship is assessed jointly with relationships for these correction factors. Eq. (3) assumes that the liquefaction triggering hazard can be completely explained by a set of five descriptive variables $\mathbf{x} = (N_{1,60}, CSR_{\sigma'_v, \alpha, M_w}, M_w, FC, \sigma'_v)$. But other variables exist, which may influence the initiation of liquefaction. Even if the selected descriptive variables were able to fully explain the

liquefaction triggering phenomenon, the adopted mathematical expression may not have the ideal form. Hence, Eq. (3) is by definition an imperfect model of the limit-state function. This is signified by the use of a superposed "hat" on g . To account for the influences of possible missing variables and the possible imperfect model form, a random model error term, ε , was introduced as given in Eq. (4).

$$g(x, \theta) = N_{1,60}(1 + \theta_1 FC) - \theta_2 \ln(M_w) - \theta_3 \ln\left(\frac{\sigma'_v}{P_a}\right) + \theta_4 FC + \theta_5 - \theta_6 \ln(CSR_{\sigma'_v, \alpha, M_w}) + \varepsilon \tag{4}$$

With the aim of producing an unbiased model (i.e., one that, on the average, makes the correct prediction), the mean of ε is set to zero, and for convenience it is assumed to be normally distributed. The standard deviation of ε , denoted σ_ε , however is unknown and must be estimated as part of the regression. The set of unknown coefficients of the model, therefore, is $\Theta = (\theta, \sigma_\varepsilon)$.

Let $x_i = (N_{1,60,i}, CSR_{\sigma'_v, \alpha, M_w,i}, M_{w,i}, FC_i, \sigma'_{v,i})$ be the values of $N_{1,60}$, CSR , M_w , FC and σ'_v for the i th case history, respectively, and ε_i be the corresponding realization of the model correction term. If the i th case history field performance is liquefied, then $g(x_i, \varepsilon_i, \theta) \leq 0$. On the other hand, if the i th case history field performance is nonliquefied, then $g(x_i, \varepsilon_i, \theta) > 0$. When $g(x_i, \varepsilon_i, \theta) \cong 0$ then the case history is defined as marginally liquefied (or marginally nonliquefied). Assuming that the Cetin et al. [4,9] database is compiled from statistically independent liquefaction field performance case histories, the likelihood function can be written as the product of the probabilities of the observations given in Eq. (5).

$$L(\theta, \sigma_\varepsilon) = \prod_{l=1}^{\text{Num. of liquefied sites}} P[g(x_l, \varepsilon_l, \theta) \leq 0] \cdot \prod_{j=1}^{\text{Num. of non-liquefied sites}} P[g(x_j, \varepsilon_j, \theta) > 0] \cdot \prod_{k=1}^{\text{Num. of marginally liquefied sites}} P[g(x_k, \varepsilon_k, \theta) \cong 0] \tag{5}$$

Suppose that $x_i = (N_{1,60,i}, CSR_{\sigma'_v, \alpha, M_w,i}, M_{w,i}, FC_i, \sigma'_{v,i})$ for each liquefaction field performance case history is exact, i.e., no measurement or estimation uncertainty is present. Then, noting that Eq. (4) has the

correction factors 0.8 and 1.2, respectively.

If $x_i = (N_{1,60,i}, CSR_{\sigma'_v, \alpha, M_w,i}, M_{w,i}, FC_i, \sigma'_{v,i})$ is inexact (uncertain), then this additional uncertainty should be included in the formulation of the likelihood function as given in Eq. (7).

$$L(\theta, \sigma_\varepsilon) = \prod_{\text{liquefied sites}} \Phi \left[-\frac{\hat{g}(x_i, \theta)}{\sigma_{\varepsilon, \text{tot}, i}} \right]^{w_{\text{liq}}} \cdot \prod_{\text{non-liquefied sites}} \Phi \left[\frac{\hat{g}(x_i, \theta)}{\sigma_{\varepsilon, \text{tot}, i}} \right]^{w_{\text{nonliq}}} \cdot \prod_{\text{marginally-liquefied sites}} \phi \left[\frac{\hat{g}(x_i, \theta)}{\sigma_{\varepsilon, \text{tot}, i}} \right] \tag{7}$$

Assuming that the mean values of the case history descriptive input parameters $N_{1,60,i}, CSR_{\sigma'_v, \alpha, M_w,i}, M_{w,i}, FC_i, \sigma'_{v,i}$ are estimated in an unbiased manner (i.e., mean choices, rather than conservative or unconservative choices, are made in case history processing) then the error terms of $N_{1,60,i}, \ln(CSR_{\sigma'_v, \alpha, M_w,i}), \ln(M_{w,i}), FC_i, \ln(\sigma'_{v,i})$ can be considered as normally distributed random variables with zero means and standard deviations $\sigma_{N_{1,60,i}}, \sigma_{\ln(CSR_{\sigma'_v, \alpha, M_w,i})}, \sigma_{\ln(M_w,i)}, \sigma_{FC,i}$ and $\sigma_{\ln(\sigma'_v,i)}$, respectively. Then the overall variance of each liquefaction field performance case history (σ_{tot}^2) is estimated as the sum of the variance of case history input parameters ($\sigma_{\text{case-history}}^2$) and model error (σ_ε^2) as given in Eq. (8).

$$\sigma_{\text{tot}, i}^2 = (\theta_7 \cdot \sigma_{\text{case-history}, i})^2 + \sigma_\varepsilon^2 \tag{8}$$

In Eq. (8), $\sigma_{\text{case-history}, i}$ represents the consolidated uncertainty of individual case history input parameters, and as discussed earlier a scaling factor of θ_7 is systematically applied to them. This factor (θ_7) is one of the regressed parameters of the overall triggering relationship. If the higher-order terms are eliminated, then $\sigma_{\text{case-history}, i}$ can be estimated as given Eq. (9).

$$\sigma_{\text{case-history}, i}^2 = (\theta_6)^2 \cdot [\text{cov}(CSR_{\sigma'_v, \alpha, M_w,i})]^2 + \sigma_{N_{1,60,i}}^2 \cdot (1 + \theta_1 \cdot FC_i)^2 + \sigma_{FC_i}^2 \cdot (\theta_1 \cdot N_{1,60,i} + \theta_4)^2 + (\theta_3)^2 \cdot [\text{cov}(\sigma'_{v,i})]^2 \tag{9}$$

Finally, the eight model coefficients (i.e.: θ_1 through θ_7 , and σ_ε) are assessed simultaneously in a single overall regression in order to maximize the likelihood function presented in Eq. (9). The resulting (new) recommended seismic soil liquefaction triggering relationships are presented in Eqs. (10) and (11) and the new model coefficients are listed in Table 7 along with CEA2004 model coefficients for comparison

$$P_L(N_{1,60}, CSR_{\sigma'_v, \alpha=0, M_w}, M_w, \sigma'_v, FC) = \Phi \left(\frac{(N_{1,60}(1 + \theta_1 \cdot FC) - \theta_6 \cdot \ln(CSR_{\sigma'_v, \alpha=0, M_w}) - \theta_2 \cdot \ln(M_w) - \theta_3 \cdot \ln\left(\frac{\sigma'_v}{P_a}\right) + \theta_4 \cdot FC + \theta_5)}{\sigma_\varepsilon} \right) \tag{10}$$

$$CRR(N_{1,60}, M_w, \sigma'_v, FC, P_L) = \exp \left[\frac{(N_{1,60}(1 + \theta_1 \cdot FC) - \theta_2 \cdot \ln(M_w) - \theta_3 \cdot \ln\left(\frac{\sigma'_v}{P_a}\right) + \theta_4 \cdot FC + \theta_5 + \sigma_\varepsilon \cdot \Phi^{-1}(P_L))}{\theta_6} \right] \tag{11}$$

normal distribution with mean $\hat{g}(x_i, \theta)$ and standard deviation σ_ε , the likelihood function Eq. (5) can be written as given in Eq. (6).

$$L(\theta, \sigma_\varepsilon) = \prod_{\text{liquefied sites}} \Phi \left[-\frac{\hat{g}(x_l, \theta)}{\sigma_\varepsilon} \right]^{w_{\text{liq}}} \cdot \prod_{\text{non-liquefied sites}} \Phi \left[\frac{\hat{g}(x_j, \theta)}{\sigma_\varepsilon} \right]^{w_{\text{nonliq}}} \cdot \prod_{\text{marginally-liquefied sites}} \phi \left[\frac{\hat{g}(x_k, \theta)}{\sigma_\varepsilon} \right] \tag{6}$$

In Eq. (6), $\Phi[\cdot]$ and $\phi[\cdot]$ are the standard normal cumulative function and the standard normal probability density functions, respectively. Also note that w_{liq} and w_{nonliq} are the sampling bias

purposes.

The new probabilistic boundary curves are shown in Fig. 4. Fig. 5 presents a direct comparison between the new triggering relationship and the previous relationship of CEA2004. These new triggering relationships will be referred to as CEA2018, hereafter.

In Eq. (10), P_L is the probability of liquefaction in decimals (i.e. $P_L = 30\%$ is input as 0.30), $CSR_{\sigma'_v, \alpha=0, M_w}$ is not "adjusted" for vertical overburden stress or magnitude/duration effects (corrections are executed within the equation itself), FC is percent fines content (by dry weight) expressed as an integer (e.g.: 12% fines is input as $FC = 12$) with the limit of $5 \leq FC \leq 35$, P_a is atmospheric pressure (1 atm =

Table 7
A comparative summary of limit state model coefficients.

Model coefficients	CEA2004	CEA2018
θ_1	0.004	0.00167
θ_2	29.530	27.352
θ_3	3.700	3.958
θ_4	0.050	0.089
θ_5	16.850	16.084
θ_6	13.320	11.771
θ_7	–	0.392
σ_c	2.70	2.95

101.3 kPa = 2116.2 psf) in the same units as the in-situ vertical effective stress (σ'_v), and Φ is the standard cumulative normal distribution. The cyclic resistance ratio, CRR, for a given probability of liquefaction can be expressed as given in Eq. (11), where

$\Phi^{-1}(P_L)$ is the inverse of the standard cumulative normal distribution (i.e. mean = 0, and standard deviation = 1). For spreadsheet construction purposes, the command in Microsoft Excel for this specific function is “NORMINV($P_L, 0, 1$)”. In Figs. 4 and 5, factor of safety (FS) values corresponding to probability of liquefaction 5%, 20%, 50%, 80%, 95% are also shown. Approximate factors of safety, FS values can be estimated by Eq. (12) based on the assumption that P_L value of 50% corresponds to a best-estimate factor of safety value equal to 1.0 and the resulting FS values for the five sets of P_L contours are also shown in Figs. 4 and 5.

$$FS = \frac{CRR(P_L = 50\%)}{CRR(P_L)} = \exp\left[\frac{(-\sigma_c \cdot \Phi^{-1}(P_L))}{\theta_6}\right] = \exp\left[\frac{(-2.95 \cdot \Phi^{-1}(P_L))}{11.771}\right] = \exp[-0.251 \cdot \Phi^{-1}(P_L)] \quad (12)$$

For the purpose of assessing the effects of sampling disparity (and weighting), the same exercise was then repeated, but this time without applying weights on non-liquefied and liquefied case history data points. Fig. 6 presents the relative positions of equi-probability (5%, 20%, 50%, 80% and 95%) liquefaction triggering contours with (solid lines) and without the weighting factors (dashed lines). Since it would be potentially over-conservative to leave the sampling disparity problem unaddressed, the model developed with weighting factors of $w_{\text{non-liquefied}} = 1.2$ and $w_{\text{liquefied}} = 0.8$ is recommended for forward engineering assessments.

5. Recommended use of the new correlations

The proposed new probabilistic correlations can be used in two ways. They can be used directly, all at once, as summarized in Eqs. (10) and (11). Alternatively, they can be used “in parts” as has been conventional for most previous, similar methods. The use of both of the alternatives in seismic soil liquefaction triggering assessments is presented in Cetin et al. [7] for an illustrative seismic soil liquefaction triggering assessment of a soil site shaken by a scenario earthquake. The protocols, which need to be followed, as well as the recommendations which guides the engineers through the procedure and “tricks” for the correct use of the methodology for forward engineering (design) assessments are discussed in the subject manuscript. Hence, the readers are referred to Cetin et al. [7] for the consistent use of the methodology, mean and uncertainty estimations of input parameters: i.e.: SPT blow-count along with Fines Content data, CSR and its input parameters of maximum ground acceleration, stress reduction (mass participation) factor r_d , moment magnitude, vertical effective and total stresses.

“In-part” use of the proposed seismic soil liquefaction triggering relationships require the application of fines, stress and magnitude correction factors (K_σ and K_{M_w}). Fig. 7 shows the regressed fines corrections for these current studies, and also for the previous triggering relationships of CEA2004. The overall average fines corrections for the

two relationships are similar, and the new fines correction relationship has a lesser dependence upon $N_{1,60}$.

Similarly, in-situ equivalent uniform $CSR_{\sigma'_v, \alpha, M_w}$ can be evaluated either based on (1) direct seismic site response analyses, or (2) direct seismic site response and soil-structure-interaction analyses, or (3) using the “simplified” approach employing Eq. (1), and the Cetin and Seed [6] r_d relationships.

$CSR_{\sigma'_v, \alpha, M_w}$ is then adjusted by the K_σ , K_α and K_{M_w} correction factors to convert overburden and static shear stresses, and duration (magnitude) to the references states of $\sigma'_v = 1$ atm, $\alpha = 0$ and $M_w = 7.5$, as given in Eqs. (13)–(15). Note that for level sites (which includes all field performance case histories in the database) the value of $K_\alpha = 1.0$.

$$CSR_{\sigma'_v=1 \text{ atm}, \alpha=0, M_w=7.5} = CSR_{\sigma'_v, \alpha, M_w} \cdot \frac{1}{K_\sigma} \cdot \frac{1}{K_{M_w}} \cdot \frac{1}{K_\alpha} \cdot \lim \quad (13)$$

$$: CSR_{\sigma'_v=1 \text{ atm}, \alpha=0, M_w=7.5} \leq 0.6$$

$$K_\sigma = \left(\frac{\sigma'_v}{P_a}\right)^{-\theta_3/\theta_6} = \left(\frac{\sigma'_v}{P_a}\right)^{-3.958/11.771} = \left(\frac{\sigma'_v}{P_a}\right)^{-0.336} ; \lim : 0.8 \leq K_\sigma \leq 1.6 \quad (14)$$

$$K_{M_w} = \left(\frac{M_w}{7.5}\right)^{-\theta_2/\theta_6} = \left(\frac{M_w}{7.5}\right)^{-27.352/11.771} = \left(\frac{M_w}{7.5}\right)^{-2.324} ; \lim : 5.5 \leq M_w \leq 8.4 \quad (15)$$

As an alternative to Eqs. (14) and (15), K_σ and K_{M_w} corrections can be employed by using Figs. 8 and 9.

Fig. 8 shows the new K_σ curve regressed from the liquefaction performance field case history database, and the lower portion of Fig. 8 shows a histogram of the distribution of case histories with different ranges of σ'_v . This field case history-based K_σ relationship is valid over the range of approximately $0.25 \text{ atm} \leq \sigma'_v \leq 1.8 \text{ atm}$. Extrapolation to higher values of σ'_v for forward engineering analyses is discussed in the companion paper of Cetin et al. [24].

The new K_σ curve is observed to be largely consistent with the CEA2004 recommendations, which were also based on regressions of field performance case histories, and at least approximately also fits laboratory cyclic simple shear test results of Cetin and Bilge [34] and is similar to a dataset of cyclic triaxial and cyclic simple shear data

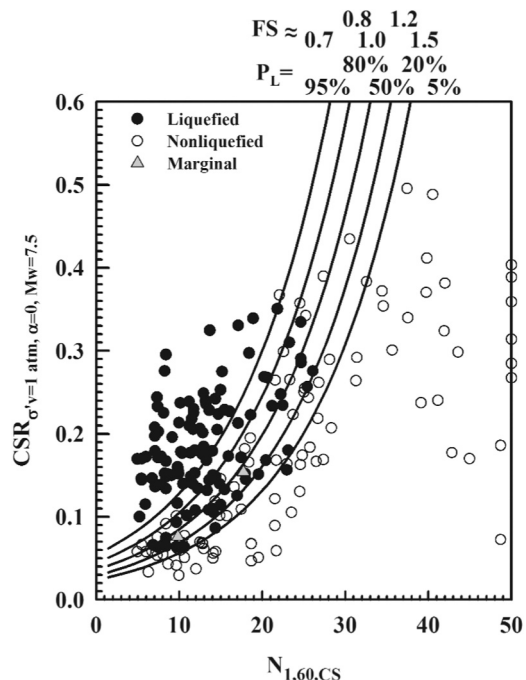


Fig. 4. New probabilistic seismic soil liquefaction triggering curves.

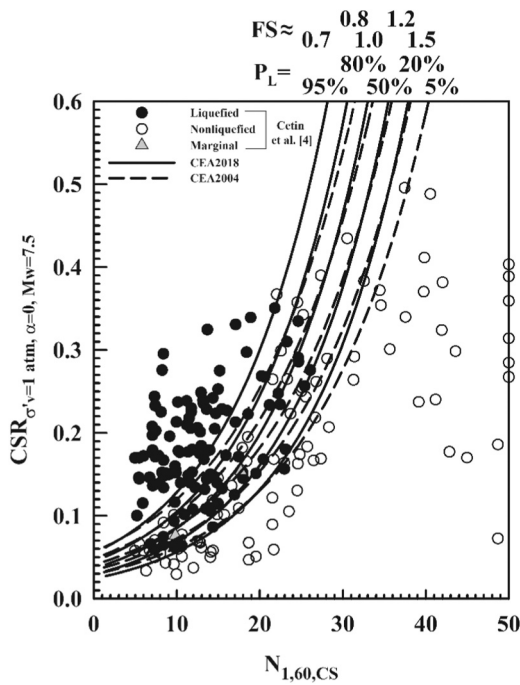


Fig. 5. Comparison between the triggering boundary curves of CEA2004 and these current studies.

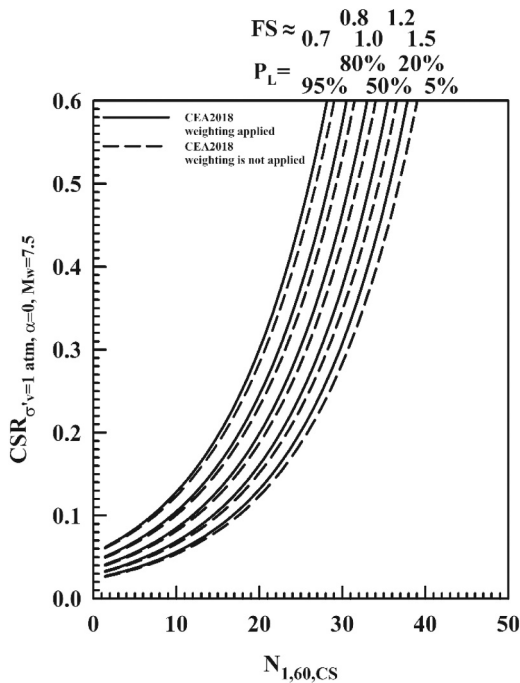


Fig. 6. Effects of implementing compensation for sampling disparity (solid lines) vs. leaving sampling disparity unaddressed.

collected and compiled by Montgomery et al. [35]. In the literature, there also exist alternative K_σ relationships which were developed on the basis of cyclic laboratory test data (e.g. Vaid et al. [36], Hynes and Olsen [37], Boulanger [31], Cetin and Bilge [34], etc.). As discussed in the recent state of the art report of NAP [3] both the case history or laboratory test data based K_σ frameworks are judged to be technically valid and their use for the stress normalization of high effective stress case history CSR values to the CSR values at the reference state of 1 atm vertical effective stress, is possible.

Fig. 9 presents the new K_{M_w} curve, which was also developed based

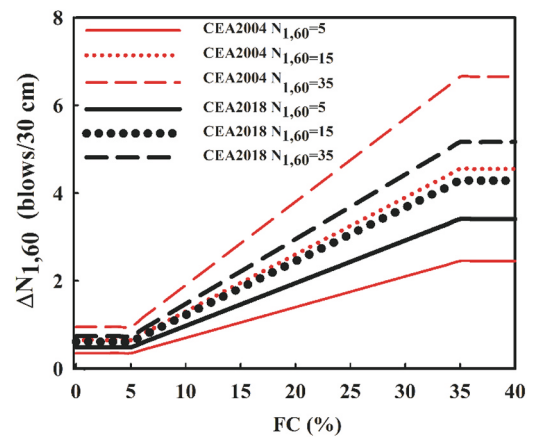


Fig. 7. Proposed $N_{1,60}$ dependent fines correction.

on the overall regression of the liquefaction triggering field performance case history database. It agrees well with the relationship of CEA2004, which was also based on regression of field case histories, and it is bound within the field K_{M_w} lower-bound of NCEER [28] (the upper bound curve of Andrus and Stokoe [42] is also presented on Fig. 9), the laboratory relationships of Idriss [38,39] and Boulanger and Idriss [22], and the shear wave velocity – based relationships of Kayen et al. [27]. Agreement between these, Seed and Idriss [40], and Cetin and Bilge [41] K_{M_w} relationships developed based on different sets of approaches is relatively good.

The resulting, fully adjusted and normalized values of $N_{1,60,cs}$ and $CSR_{\sigma'_{v'}=1 \text{ atm}, \alpha=0, M_w=7.5}$ can then be used, with Fig. 4, to assess the probability of initiation of liquefaction. For “deterministic” evaluation of liquefaction resistance Eq. (12) can be used to approximate an acceptable factor of safety.

6. Conclusions

The preparation of the report by the National Academies of Sciences, Engineering, and Medicine on the “State of the Art and Practice in the Assessment of Earthquake-Induced Soil Liquefaction and Its Consequences” provided the authors the motivation and impetus to update the SPT-based relationship of CEA2004 and cast a new probabilistic triggering relationship based upon the updated field database. New probabilistic and deterministic liquefaction triggering curves are proposed based on the most recent case history database of Cetin et al.

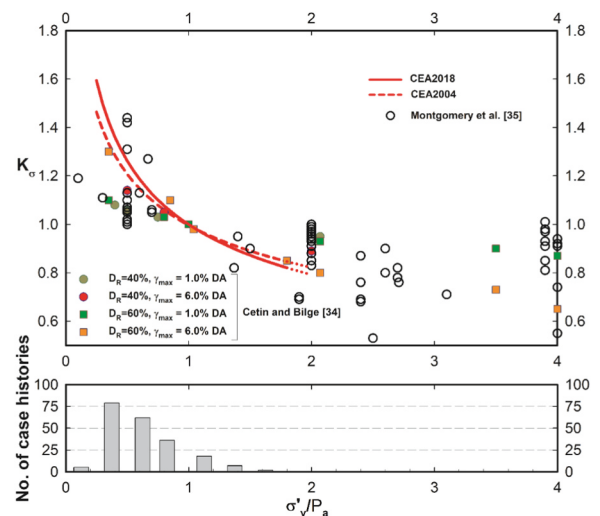


Fig. 8. Newly regressed K_σ corrections compared with available cyclic laboratory test data.

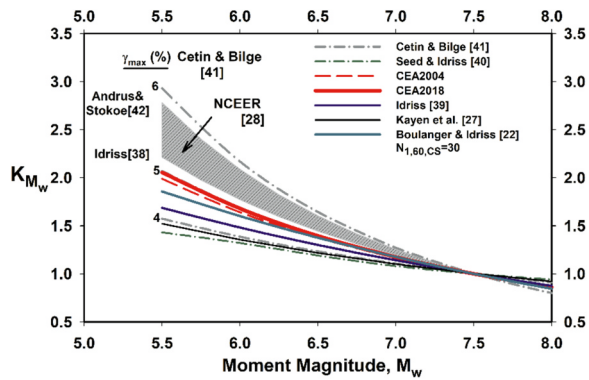


Fig. 9. Newly regressed K_{M_w} corrections compared with available literature.

[4,9]. Maximum likelihood models for assessment of seismic soil liquefaction initiation are presented, and in their development the relevant uncertainties including (a) measurement / estimation uncertainties of input parameters, (b) limit state model imperfection, (c) statistical uncertainty, and (d) uncertainties arising from inherent variability were addressed.

The use of site-specific and event-specific seismic site response-based calculations of CSR, and of compatible unbiased (median) probabilistic r_d relationships based on representative suites of site conditions results in triggering relationships that are therefore unbiased with respect to use in conjunction with either (1) direct seismic site response analyses, or site response and soil-structure interaction analyses, for evaluation of in-situ CSR, or (2) improved “simplified” assessment of in-situ CSR in forward engineering analyses.

The new models provide an improved basis for engineering assessment of the likelihood of liquefaction initiation. The proposed models deal explicitly with the issues of (1) fines content (FC), (2) magnitude (duration) effects (i.e.: K_{M_w} correction), and (3) effective overburden stress effects (i.e.: K_σ correction). These correction factor relationships are all developed based on regression of the entire field case history database. As a result, the overall triggering relationships provide both (1) an unbiased (median) basis for evaluation of liquefaction initiation hazard, and (2) a basis for assessment of overall model uncertainty. Overall uncertainty in application of these new correlations to field problems is driven by the difficulties/uncertainties associated with project-specific engineering assessment of the “loading” and “resistance” variables. In the estimation of these loading and resistance terms, the need to use a series of corrections and normalizations remains at the heart of the triggering assessment. The objective of this updated set of correlations is to provide an unbiased set of liquefaction triggering relationships, normalized at $\sigma'_v = 1$ atm, $M_w = 7.5$ and $\alpha = 0$. These relationships are recommended to be used for either probabilistic or deterministic assessment of seismic soil liquefaction triggering. The use of them beyond their recommended limits by simple extrapolation techniques without additional, project specific engineering assessments and/or laboratory testing-based confirmations may lead to unconservatively biased predictions; hence it is strongly discouraged.

Acknowledgements

The authors are deeply grateful to the many engineers and researchers who developed the field case history data upon which these types of correlations are based. We are also grateful to the many engineers, colleagues and our anonymous Reviewers, who encouraged this current work, and whose discussions and comments were of great value.

Appendix A. Supplementary material

Supplementary data associated with this article can be found in the online version at doi:10.1016/j.soildyn.2018.09.012.

References

- [1] Cetin KO, Seed RB, Moss RES, Der Kiureghian AK, Tokimatsu K, Harder LF, et al. Field performance case histories for SPT-based evaluation of soil liquefaction triggering hazard, (Geotechnical Research Report No. UCB/GT-2000/09) Berkeley, CA: Dept. of Civil and Environmental Engineering, University of California at Berkeley; 2000.
- [2] Cetin KO, Seed RB, Der Kiureghian A, Tokimatsu K, Harder Jr LF, Kayen RE, et al. SPT-based probabilistic and deterministic assessment of seismic soil liquefaction potential. *ASCE J Geotech Geoenviron Eng* 2004;130(12):1314–40.
- [3] NAP. State of the art and practice in the assessment of earthquake-induced soil liquefaction and its consequences. National Academies of Sciences, Engineering, and Medicine; Washington, DC: The National Academies Press; 2016. <https://dx.doi.org/10.17226/23474>.
- [4] Cetin KO, Seed RB, Kayen RE, Moss RES, Bilge HT, Ilgac M, et al. Summary of SPT-based field case history data of the updated 2016 Database. (Report no: METU/GTENG 08/16-01) METU Soil Mechanics and Foundation Engineering Research Center; 2016.
- [5] Cetin KO. Reliability-based assessment of seismic soil liquefaction initiation hazard. Dissertation submitted in partial fulfillment of the requirement for the degree of Doctor of Philosophy, University of California at Berkeley; 2000.
- [6] Cetin KO, Seed RB. Nonlinear shear mass participation factor, r_d for cyclic shear stress ratio evaluation. *Soil Dyn Earthq Eng J* 2004;24(2):103–13.
- [7] Cetin KO, Seed RB, Kayen RE, Moss RES, Bilge HT, Ilgac M, et al. The use of the SPT-based seismic soil liquefaction triggering evaluation methodology in engineering hazard assessments. *Methods X* 2018. [In preparation].
- [8] Japan Road Association Design Specifications for Highway Bridges; 2002.
- [9] Cetin KO, Seed RB, Kayen RE, Moss RES, Bilge HT, Ilgac M, et al. Dataset on SPT-based seismic soil liquefaction. *Data Brief* 2018;20:544–8. Elsevier.
- [10] Idriss IM, Boulanger RW. SPT-based liquefaction triggering procedures. (Report UCD/CGM-10/02) Davis, CA: Center for Geotechnical Modeling, Department of Civil and Environmental Engineering, University of California; 2010. p. 136.
- [11] Idriss IM, Boulanger RW. Examination of SPT-based liquefaction triggering correlations. *Earthq Spectra* 2012;28(3):989–1018.
- [12] Seed HB, Tokimatsu K, Harder LF, Chung RM. The influence of SPT procedures in soil liquefaction resistance evaluations. (Earthquake Engineering Research Center Report No. UCB/EERC-84/15) Berkeley, CA: Dept. of Civil and Environmental Engineering, University of California at Berkeley; 1984.
- [13] Bennett MJ, Ponti DJ, Tinsley JC, Holzer TL, Conaway CH. Subsurface geotechnical investigations near sites of ground deformations caused by the 17 January 1994 Northridge California Earthquake. (Open File Report 1998). Department of Interior U.S. Geological Survey, p. 98–373.
- [14] Kayen R. Seismic displacement of gently-sloping coastal and marine sediment under multidirectional earthquake loading. *Eng Geol* 2016. <https://doi.org/10.1016/j.enggeo.2016.12.009>.
- [15] Youd TL. Discussion of “examination and reevaluation of SPT-based liquefaction triggering case histories” by Ross W. Boulanger, Daniel W. Wilson, and I.M. Idriss. *J Geotech Geoenviron Eng* 2013;138(8):898–909.
- [16] Wayne AC, Donald OD, Jeffrey PB, Hassen H. Direct measurement of liquefaction potential in soils of Monterey County, California. In: Holzer TL, editor. *The Loma Prieta, California, Earthquake of October 17, 1989: Liquefaction*. Washington D.C.: U.S. Government Printing Office; 1998. p. B181–208.
- [17] Engdahl ER, Villaseñor A. Global seismicity: 1900–1999. International handbook of earthquake and engineering seismology. International Association of Seismology and Physics of the Earth's Interior, Committee on Education; 81A; 2002. p. 665–90.
- [18] NGA Flatfiles. <http://peer.berkeley.edu/ngawest2/databases/>; 2015.
- [19] Incorporated Research Institutions for Seismology (IRIS) Seismo Archives, <http://ds.iris.edu/seismo-archives/>; 2004.
- [20] Ide S, Takeo M. The dynamic rupture process of the 1993 Koshiro-oki earthquake. *J Geophys Res* 1996;101(B3):5661–75.
- [21] Iai S, Tsuchida H, Koizumi K. A liquefaction criterion based on field performances around seismograph stations. *Soils Found* 1989;29(2):52–68.
- [22] Boulanger RW, Idriss IM. CPT and SPT based liquefaction triggering procedures. (Report No. UCD/CGM-14/01). Davis, CA: Center for Geotechnical Modeling, Department of Civil and Environmental Engineering, University of California; 2014. p. 134.
- [23] Seed HB, Tokimatsu K, Harder LF, Chung RM. The influence of SPT procedures in soil liquefaction resistance evaluations. *J Geotech Eng ASCE* 1985;111(12):1425–45.
- [24] Cetin KO, Seed RB, Kayen RE, Moss RES, Bilge HT, Ilgac M, et al. Examination of differences between three SPT-based seismic soil liquefaction triggering relationships. *Soil Dyn Earthq Eng* 2018;113:75–86. Elsevier.
- [25] Idriss IM, Sun JI. User's manual for SHAKE91, a computer program for conducting equivalent linear seismic response analyses of horizontally layered soil deposits program modified based on the original SHAKE program published in December 1972 by Schnabel, Lysmer and Seed; 1992.
- [26] Cetin KO, Seed RB. Earthquake-induced nonlinear shear mass participation factor (r_d). (Geotechnical Research Rept. No. UCB/GT-2000/08). Berkeley, CA: Dept. of Civil and Environmental Engineering, University of California at Berkeley; 2000.

- [27] Kayen R, Moss R, Thompson E, Seed R, Cetin K, Kiureghian A, et al. Shear-wave velocity-based probabilistic and deterministic assessment of seismic soil liquefaction potential. *J Geotech Geoenviron Eng* 2013;407–19. [https://doi.org/10.1061/\(ASCE\)GT.1943-5606.0000743](https://doi.org/10.1061/(ASCE)GT.1943-5606.0000743).
- [28] NCEER. In: Youd TL, Idriss IM, editors. Proceedings of the NCEER workshop on evaluation of liquefaction resistance of soils (Technical Report No. NCEER-97-0022). National Center for Earthquake Engineering Research, SUNY, Buffalo; 1997.
- [29] Youd TL, Idriss IM, Andrus RD, Arango I, Castro G, Christian JT, et al. Liquefaction resistance of soils. Summary report from the 1996 NCEER and 1998 NCEER/NSF workshops on evaluation of liquefaction resistance of soils. *J Geotech Geoenviron Eng* 2001;127(10):817–33.
- [30] Liao SSC, Whitman RV. Overburden correction factor OS for SPT in sand. *J Geotech Eng* 1986;112(3):373–7.
- [31] Boulanger RW. High overburden stress effects in liquefaction analyses. *J Geotech Geoenviron Eng ASCE* 2003;129(12):1071–82.
- [32] Sancio RB, Bray JD. An assessment of the effect of rod length on SPT energy calculations based on measured field data. *Geotech Test J ASTM* 2005;28(1):1–9. [Paper GTJ11959].
- [33] Cetin KO, Der Kiureghian A, Seed RB. Probabilistic models for the initiation of seismic soil liquefaction. *J Struct Saf* 2002;24(1):67–82.
- [34] Cetin KO, Bilge HT. Stress scaling factors for seismic soil liquefaction engineering problems: a performance-based approach. In: Proceedings of the international conference on earthquake geotechnical engineering from case history to practice in honor of Prof. Kenji Ishihara, Istanbul, Turkey; 2013.
- [35] Montgomery J, Boulanger RW, Harder Jr. LF. Examination of the K_{σ} overburden correction factor on liquefaction resistance. *J Geotech Geoenviron Eng* 2014. [https://doi.org/10.1061/\(ASCE\)GT.1943-5606.0000743](https://doi.org/10.1061/(ASCE)GT.1943-5606.0000743).
- [36] Vaid YP, Chern JC, Tumi H. Confining pressure, grain angularity and liquefaction. *J Geotech Eng ASCE* 1985;111(10):1229–35.
- [37] Hynes ME, Olsen RS. Influence of confining stress on liquefaction. *Physics and Mechanics of Soil Liquefaction*. Balkema, Rotterdam; 1999. p. 145–51.
- [38] Idriss IM. Seed memorial lecture. University of California at Berkeley; 1995.
- [39] Idriss IM. An update to the Seed-Idriss simplified procedure for evaluating liquefaction potential. (Publication No. FHWA-RD-99-165). In: Proceedings of the TRB workshop on new approaches to liquefaction, Federal Highway Administration; 1999.
- [40] Seed HB, Idriss IM. Ground motion and soil liquefaction during earthquakes. Oakland, Calif.: Earthquake Engineering Research Institute Monograph; 1982.
- [41] Cetin KO, Bilge HT. Performance-based assessment of magnitude (duration) scaling factors. *J Geotech Geoenviron Eng ASCE* 2012;138(3):324–34.
- [42] Andrus RD, Stokoe KH II. Liquefaction resistance based on shear wave velocity. In: Proceedings of the NCEER workshop on evaluation of liquefaction resistance of soils. State Univ. of New York, Buffalo; 1997. p. 89–128.